Recreating a Functional Ancestral Archosaur Visual Pigment

Belinda S. W. Chang, Karolina Jönsson,* Manija A. Kazmi,* Michael J. Donoghue,† and Thomas P. Sakmar**

*Laboratory of Molecular Biology & Biochemistry, The Rockefeller University, New York; and †Department of Ecology & Evolutionary Biology, Yale University

The ancestors of the archosaurs, a major branch of the diapsid reptiles, originated more than 240 MYA near the dawn of the Triassic Period. We used maximum likelihood phylogenetic ancestral reconstruction methods and explored different models of evolution for inferring the amino acid sequence of a putative ancestral archosaur visual pigment. Three different types of maximum likelihood models were used: nucleotide-based, amino acid–based, and codon-based models. Where possible, within each type of model, likelihood ratio tests were used to determine which model best fit the data. Ancestral reconstructions of the ancestral archosaur node using the best-fitting models of each type were found to be in agreement, except for three amino acid residues at which one reconstruction differed from the other two. To determine if these ancestral pigments would be functionally active, the corresponding genes were chemically synthesized and then expressed in a mammalian cell line in tissue culture. The expressed artificial genes were all found to bind to 11-*cis*-retinal to yield stable photoactive pigments with λ_{max} values of about 508 nm, which is slightly redshifted relative to that of extant vertebrate pigments. The ancestral archosaur pigments also activated the retinal G protein transducin, as measured in a fluorescence assay. Our results show that ancestral genes from ancient organisms can be reconstructed de novo and tested for function using a combination of phylogenetic and biochemical methods.

Introduction

Visual pigments trigger the critical first step in the biochemical cascade of vision (Stryer 1986). Several key features of visual pigments have been conserved throughout evolution. For example, a retinylidene chromophore is linked covalently via a Schiff base to a highly conserved lysine residue in all cases. But visual pigments have also evolved to perform specialized functions, such as color vision and scotopic (dim light) vision. Rhodopsin is specialized for high sensitivity under conditions of dim light. It has evolved several unique photochemical and biochemical properties, including an unusually high quantum efficiency, an extremely low level of biochemical noise in darkness, and an absorption maximum at about 500 nm (Menon, Han, and Sakmar 2001).

One experimental approach used in studies of molecular evolution is the use of phylogenetic methods to infer ancestral sequences of biological molecules with the aim of recreating extinct genes or proteins in the laboratory (Chang and Donoghue 2000). This approach shows much promise for investigating the function and evolution of ancient proteins (Malcolm et al. 1990; Adey et al. 1994; Chandrasekharan et al. 1996; Dean and Golding 1997; Bishop, Dean, and Mitchell-Olds 2000), and perhaps even the organisms in which they existed (Jermann et al. 1995; Messier and Stewart 1997; Nei, Zhang, and Yokoyama 1997; Boissinot et al. 1998; Galtier, Tourasse, and Gouy 1999). But in taking these studies of ancestral proteins into the laboratory, few experimental studies have explored the use of maximum likelihood methods of ancestral reconstruction, particularly in the light of the plethora of likelihood models now available. Using maximum likelihood methods (Felsenstein 1981; Yang, Kumar, and Nei 1995) we explored different models for reconstructing an ancestral archosaur rhodopsin. Once inferred, the phylogenetically reconstructed archosaur rhodopsin gene sequences were then synthesized, expressed, and assayed for function in the laboratory. The ancestral archosaurs were chosen as a test case for this type of molecular paleontological approach for two reasons. First, although the archosaur lineage gave rise to some of the largest reptiles to walk the earth, including the late Cretaceous carnivorous dinosaurs, little is known yet of the physiology and behavior of their ancestors. Because visual pigments constitute the critical first step in the visual phototransduction cascade in the eye and rhodopsin in particular is essential for vision at low light levels, recreating the inferred visual pigments of the archosaur ancestors in the laboratory should be an important initial step toward a better understanding of their visual capabilities that is difficult to obtain using other means. Second, divergences among extant archosaur rhodopsin protein sequences are no more than 16%, levels within the range at which likelihood methods of ancestral reconstruction should work reasonably well.

Key words: phylogenetic ancestral reconstruction, rhodopsin, biochemical evolution, vertebrate vision G protein–coupled receptor.

Address for correspondence and reprints: Thomas P. Sakmar, Laboratory of Molecular Biology & Biochemistry, Howard Hughes Medical Institute, The Rockefeller University, 1230 York Avenue, Box 284, New York, New York 10021. E-mail: sakmar@mail.rockefeller.edu or changb@mail.rockefeller.edu.

Mol. Biol. Evol. 19(9):1483–1489. 2002
© 2002 by the Society for Molecular Biology and Evolution. ISSN: 0737-4038

Materials and Methods

Ancestral Reconstruction

Thirty vertebrate rhodopsin nucleotide sequences were obtained from GenBank, aligned with ClustalW, and adjusted by eye to ensure the alignment of structurally important amino acids and that no gaps existed within codons. Because the amino acids at the extreme ends of rhodopsin (21 amino acids at the N-terminus and 25 amino acids after the palmitoylation site at the C-terminus) are not thought to be important in determining any aspect of either photon absorption or trans-

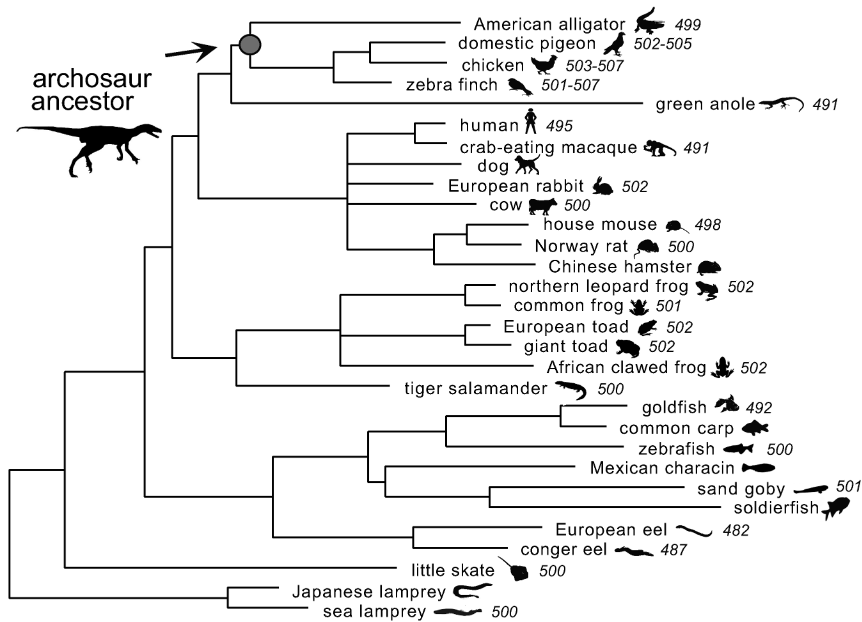

FIG. 1.—Vertebrate phylogeny used for ancestral sequence reconstruction of the archosaur node, with approximate λ_{max} for extant rhodopsins indicated in italics. References for rhodopsin genes and spectral measurements are as follows: American alligator, *Alligator mississippiensis* (Lythgoe 1972; Smith et al. 1995*a*); pigeon, *Columbia livia* (Bowmaker et al. 1997; Kawamura, Blow, and Yokoyama 1999); chicken, *Gallus gallus* (Takao, Yasui, and Tokunaga 1988; Bowmaker et al. 1997; Heath et al. 1997); zebra finch, *Taeniopygia guttata* (Bowmaker et al. 1997; Yokoyama, Blow, and Radlwimmer 2000); green anole, *Anolis carolinensis* (Kawamura and Yokoyama 1998); human, *Homo sapiens* (Nathans, Thomas, and Hogness 1984; difference spectrum); crab eating macaque, *Macaca fascicularis* (Baylor, Nunn, and Schnapf 1984; Schnapf et al. 1988; Nickells et al. 1995); dog, *Canis familiaris* (Kylma et al. 1997); European rabbit, *Oryctolagus cuniculus* (Lythgoe 1972; Smith et al. 1995*b*); cow, *Bos taurus* (Nathans and Hogness 1983); mouse, *Mus musculus* (Lythgoe 1972; Baehr et al. 1988); Norway rat, *Rattus norvegicus* (Z46957; Crouch 1976); Chinese hamster, *Cricetulus griseus* (Gale, Tobey, and D'Anna 1992); Northern leopard frog, *Rana pipiens* (Pittler, Fliesler, and Baehr 1992; Fyhrquist et al. 1998*b*); common frog, *Rana temporaria* (Fyhrquist et al. 1998*a*); European toad, *Bufo bufo* (Fyhrquist et al. 1998*b*); giant toad, *Bufo marinus* (Fyhrquist et al. 1998*b*); African clawed frog, *Xenopus laevis* (Saha and Grainger 1993; Koskelainen et al. 2000); tiger salamander, *Ambystoma tigrinum* (Makino et al. 1999); goldfish, *Carassius auratus* (Johnson et al. 1993); common carp, *Cyprinus carpio* (Tsai et al. 1994); zebrafish, *Danio rerio* (Lythgoe 1972; Vihtelic, Doro, and Hyde 1999); Mexican characin, *Astyanax fasciatus* (Yokoyama, Knox, and Yokoyama 1995); sandgoby, *Pomatoschistus minutus* (Archer, Lythgoe, and Hall 1992); soldierfish, *Myripristis berndti* (U57538); European eel, *Anguilla anguilla* (Archer, Hope, and Partridge 1995); conger eel, *Conger conger* (Archer and Hirano 1996); skate, *Raja erinacea* (Cornwall et al. 1989; O'Brien, Ripps, and Al-Ubaidi 1997); Japanese lamprey, *Lampetra japonica* (Hisatomi et al. 1991); sea lamprey, *Petromyzon marinus* (Harosi and Kleinschmidt 1993; Zhang and Yokoyama 1997). All measurements are for A1 pigments.

ducin activation and are more problematic to align with confidence, they were excluded from the ancestral reconstruction analysis (with corresponding residues from bovine rhodopsin used for the synthetic archosaur gene). The aligned vertebrate rhodopsin sequences were used to reconstruct the ancestral archosaur sequence using the phylogeny in figure 1, which reflects current understanding of systematic relationships among the major vertebrate lineages (Carroll 1997; de Jong 1998).

Ancestral reconstructions of the archosaur node were performed using maximum likelihood methods (Felsenstein 1981; Yang, Kumar, and Nei 1995), as implemented in the PAML program (Yang 1997). Marginal posterior probabilities at each site were also calculated in this program. It is important to note that these posterior probabilities are computed using the empirical Bayes approach, which does not account for errors in the parameter estimates or in the phylogeny itself. Where possible, pairwise likelihood ratio tests were used to assess among nested models which best fit the data at hand, a common approach for identifying models for use in likelihood analyses (Navidi, Churchill, and von Haeseler 1991; Yang, Goldman, and Friday 1994; Sullivan and Swofford 1997).

Synthetic Gene Design, Construction, and Expression

The artificial archosaur gene was synthesized in large fragments (168 to 230-mers) on a solid-phase oligonucleotide synthesizer (Applied Biosystems, model 392). The synthesized fragments were amplified using the *Pfu* polymerase (Stratagene), cloned into the pCR-Blunt vector (Invitrogen), pieced together using unique restriction sites, and then cloned into a mammalian expression vector (pMT). The artificial archosaur gene was expressed and purified by previously described methods (Han et al. 1996), essentially by transient transfection into COS cells using Lipofectamine Plus (Life Technologies), harvested after 48 h, regenerated in 5 μM 11-*cis* retinal, solubilized in 1% *n*-dodecyl-β-D-maltoside detergent, and immunoaffinity purified using the 1D4 monoclonal antibody. Absorbance spectroscopy was performed at 25°C using a Perkin-Elmer Lambda 800 spectrophotometer, using quartz cuvettes with a 1-cm pathlength. Transducin fluorescence was monitored at 10°C using an SPEX spectrofluorometer equipped with a Xenon arc lamp by methods described previously (Marin et al. 2000).

Table 1
Maximum Likelihood Scores and Likelihood Ratio Tests

Nucleotide	Likelihood Scores	Likelihood Ratio Tests	
		GTR + Γ	HKY85 + Γ
JC69 + Γ	−13,248	703.4* (8)	694.2* (4)
K80 + Γ	−12,964	134.4* (7)	125.2* (3)
F81 + Γ	−13,184	574.0* (5)	564.8* (1)
HKY85 + Γ	−12,901	9.2 (4)	NA
GTR + Γ	−12,897	NA	NA
Codon		F61 + Γ	
F1/61 + Γ	−11,784	719.9* (60)	
F1 × 4 + Γ	−11,698	547.4* (57)	
F3 × 4 + Γ	−11,572	296.6* (51)	
F61 + Γ	−11,424	NA	
Amino acid			
Poisson + F + Γ	−5,065		
MTMAM + F + Γ	−4,715		
Dayhoff78 + F + Γ	−4,607		
Jones92 + **F** + Γ	−4,584		

NOTE.—Likelihood ratio tests are pairwise comparisons to the model listed at the top of the column. Significance of the likelihood ratio test statistic (2ΔL) is approximated using the $\chi^2_{([df])}$ distribution, with degrees of freedom (indicated in parentheses) equal to the difference in number of parameters between the two models. Best fitting model of each type indicated in **bold**. * $P < 0.001$. NA, not applicable.

Results and Discussion

Reconstructions of the ancestral archosaur rhodopsin were performed using the data set of vertebrate rhodopsin genes available in GenBank and a phylogeny (fig. 1) that reflects current understanding of systematic relationships among the major vertebrate lineages (Carroll 1997; de Jong 1998). Phylogenetic reconstructions using model-based methods such as maximum likelihood are known to be sensitive to the assumptions of the particular model used in the analysis. Oversimplified models can yield misleading phylogenetic reconstructions (Cao et al. 1994; Huelsenbeck 1997) and may also be problematic when reconstructing ancestral states (Chang and Donoghue 2000). Therefore, we performed ancestral reconstructions using several models for each of the three types of reconstructions (nucleotide-based, amino acid–based, and codon-based). To determine which model of each type provided the best fit to the data, likelihood ratio tests (Navidi, Churchill, and von Haeseler 1991; Yang, Goldman, and Friday 1994) were carried out among pairs of nested models (table 1). Among nucleotide reconstructions, although GTR+Γ (Yang 1994) gave the highest overall likelihood score, it was not significantly better than HKY+Γ ($P = 0.33$; Hasegawa, Kishino, and Yano 1985), which in turn was significantly better than all simpler models tested. For codon-based reconstructions (Goldman and Yang 1994; Muse and Gaut 1994), the most parameter-rich model in which all the codon frequencies are allowed to vary, F61+Γ, was significantly better than simpler models tested. Among the amino acid models shown in table 1, which differ only in the fixed substitution rate matrices, Jones+F+Γ (Jones, Taylor, and Thornton 1992) gave the highest likelihood score. For all models tested, eliminating the Γ distribution, which accounts for among-site rate heterogeneity, resulted in a significantly worse fit to the data (HKY: $2\Delta L = 2824.6$, $\chi^2_{([1])} = 6.63$, $P < 0.001$; F61: $2\Delta L = 442.5$, $\chi^2_{([1])} = 6.63$, $P < 0.001$; Jones: $2\Delta L = 448.8$, $\chi^2_{([1])} = 6.63$, $P < 0.001$). Not allowing amino acid frequencies to vary in the Jones+F+G model also proved to be significantly worse ($2\Delta L = 110.7$, $\chi^2_{([19])} = 36.2$, $P < 0.001$).

For the three best-fitting models, likelihood reconstructions of the ancestral archosaur rhodopsin were found to be in agreement at all but three amino acid sites (positions 213, 217, and 218), at which one of the three reconstructions differed from the other two. At position 213, the HKY+Γ model gave Ile instead of Thr; at 217, Jones+F+Γ gave Ala instead of Thr; and at 218, Jones+F+Γ gave Ile instead of Val. In designing the synthetic archosaur gene shown in figure 2, the residue that agreed in two of the reconstructions was chosen; in fact, posterior probabilities for this residue tended to be higher than that for the alternative reconstructions (F61+Γ model: T213 (0.85), T217 (0.82), V218 (0.76); HKY+Γ model: I213 (0.60), T217 (0.86), V218 (0.75); Jones+F+Γ model: T213 (0.71), A217 (0.39), I218 (0.62)). Note that across all reconstructed sites, marginal posterior probabilities tended to be above 0.9 for the best-fitting models (fig. 2, inset). On the basis of the crystal structure of bovine rhodopsin (Palczewski et al. 2000), amino acid side chains at positions 213, 217, and 218 are expected to reside in the fifth transmembrane helix facing the bilayer lipid and might not be expected to significantly affect function, particularly in terms of spectral sensitivity and second-messenger activation. To test whether this is the case, we also synthesized a series of archosaur rhodopsin variants that contained the alternate amino acid reconstructions at the three sites (single mutants T213I, T217A, V218I, as well as a triple mutant incorporating all three substitutions).

The reconstructed ancestral archosaur rhodopsin amino acid sequence shown in figure 2 was used to design an artificial gene, which was synthesized in large fragments (168- to 230-mers) on a solid-phase oligonucleotide synthesizer. The synthesized fragments were amplified using the *Pfu* polymerase, cloned into the pCR-Blunt vector, pieced together using unique restriction sites, and cloned into a mammalian expression vector (pMT). This artificially synthesized ancestral archosaur gene was then transfected into monkey kidney (COS-1) cells, harvested, regenerated with 11-*cis* retinal in the COS cell membranes, solubilized, and purified (Ferretti et al. 1986; Chang, Kazmi, and Sakmar 2002).

The purified ancestral archosaur rhodopsin bound to 11-*cis* retinal to produce a stable pigment with a visible absorption maximum at 508 nm (fig. 3*A*), which is redshifted from that of most mammalian and fish rhodopsins but within the higher end of the range of values reported for reptiles and particularly birds, which tend to have longer wavelength–absorbing rhodopsins (see fig. 1). Upon bleaching with light, the visible absorption peak shifted to 383 nm, which is characteristic of the active conformation of metarhodopsin II (inset, fig. 3*A*). To determine if the light-activated conformation of the ancestral archosaur rhodopsin was functionally active, a

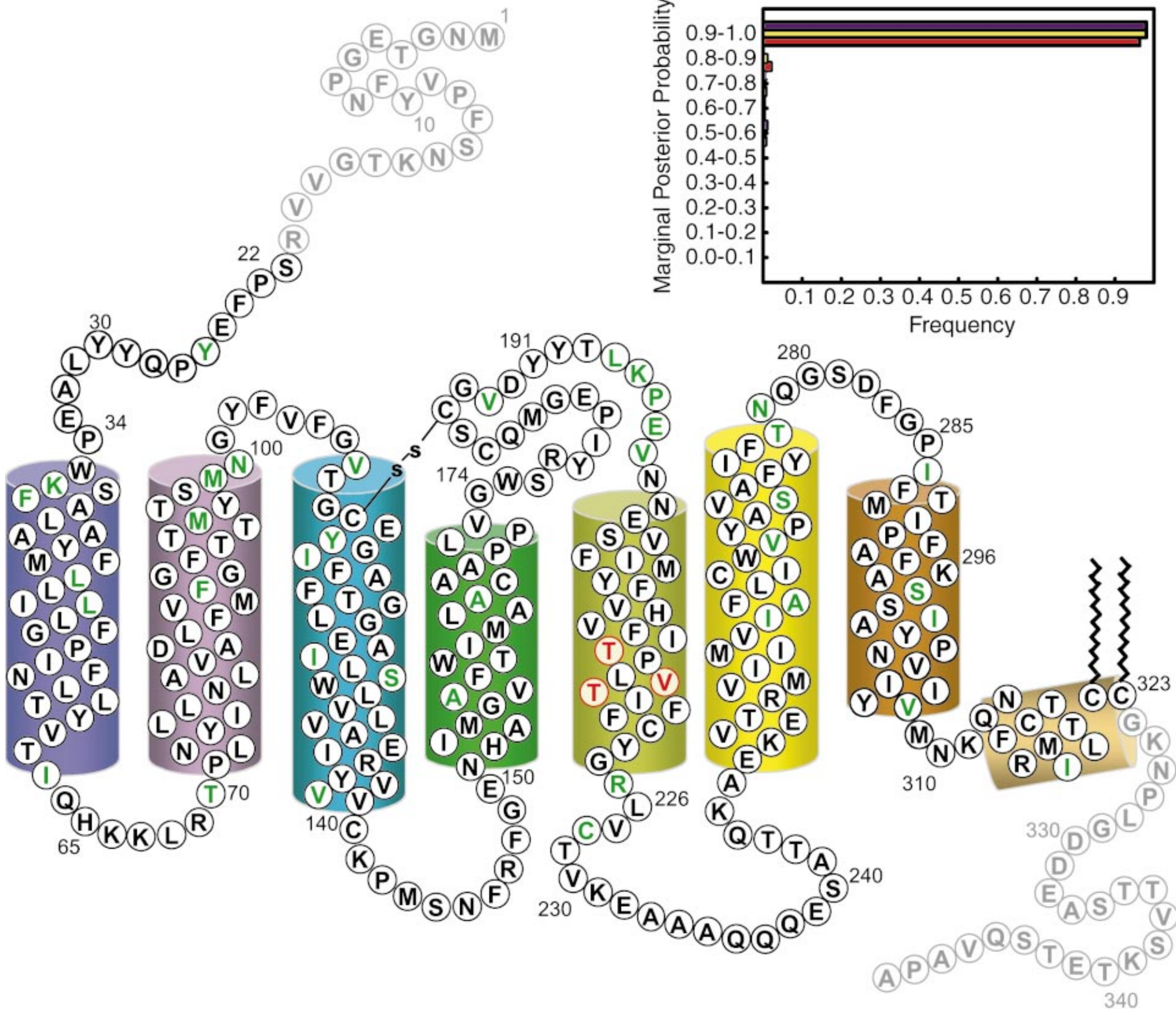

FIG. 2.—Protein sequence of the reconstructed ancestral archosaur rhodopsin drawn as a schematic on the basis of the crystal structure for bovine rhodopsin (Palczewski et al. 2000). Sites that differ among the best three reconstructions, for which variants were also synthesized, are marked in red. The 38 residues that differ from bovine or alligator rhodopsin are marked in green. Inset, frequencies of marginal posterior probabilities calculated for the most likely amino acid reconstruction at each site of the ancestral archosaur rhodopsin sequence. These posterior probabilities, which represent the likelihood of having reconstructed the correct amino acid, under the assumptions of the model used, were calculated for the best-fitting nucleotide (HKY+Γ, purple bars), codon (F61+Γ, yellow bars), and amino acid (Jones+F+Γ, red bars) models.

fluorescence assay was used to measure guanine-nucleotide uptake by the heterotrimeric G-protein transducin. The photolyzed archosaur pigment activated transducin at a rate similar to that of bovine rhodopsin (86% normalized relative to bovine rhodopsin; fig. 3*B*). Similar experiments were carried out on the ancestral archosaur rhodopsin variants (T213I, T217A, and V218I), which represent all possible alternate reconstructions. These variants showed similar results both in terms of spectral properties (λ_{max} = 508 for all three) and transducin activation rates (83%, 74%, and 79%, respectively). A triple-replacement variant was also found to have spectral properties similar to the archosaur rhodopsin (λ_{max} = 509).

These results indicate that the ancestral archosaur rhodopsin synthesized in the laboratory is able to activate the G-protein transducin in much the same way as bovine rhodopsin when assayed directly and that its spectrum is slightly redshifted. Moreover, at this level of divergence alternate amino acid reconstructions generated by different likelihood models, which were also synthesized and expressed, displayed similar functional characteristics. This indicates that archosaurs may have had a class of visual pigments that would support dim-light vision, which is consistent with the intriguing possibility that nocturnal, not diurnal, life histories may have been the ancestral state in amniotes (Gauthier 1994), though further studies will be needed to clarify this issue.

Fossils preserved well enough to shed light on physiology and behavior are extremely rare (Ruben et al. 1999; Fisher et al. 2000). Attempts to amplify ancient

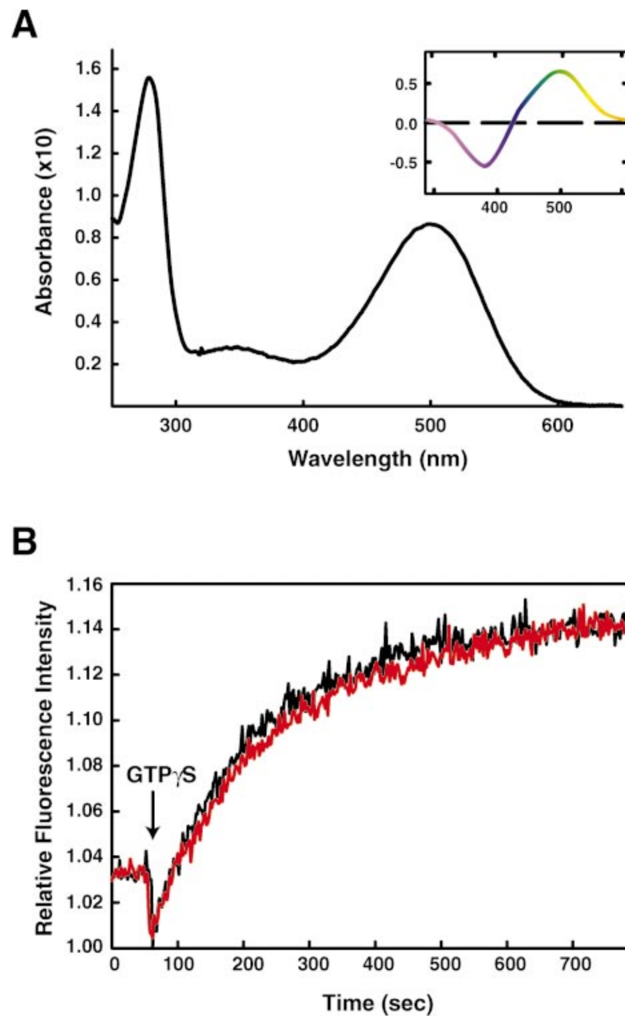

FIG. 3.—In vitro expression of the artificial ancestral archosaur rhodopsin gene. (*A*) Dark absorption spectrum for the archosaur pigment recorded using a Perkin-Elmer spectrophotometer (model 800) at 25°C. Inset, a difference spectrum generated by taking an absorbance spectrum after bleaching with a fiber optic lamp equipped with a long-pass filter (>495 nm) for 30 s and subtracting it from the dark spectrum. Ancestral archosaur rhodopsin was expressed by transient transfection into COS cells using Lipofectamine Plus (Life Technologies), harvested after 48 h, regenerated in 5 μM 11-*cis* retinal, solubilized in 1% *n*-dodecyl-β-D-maltoside detergent (50 mM Tris pH 6.8, 100 mM NaCl, 1 mM $CaCl_2$), and immunoaffinity purified using the 1D4 monoclonal antibody. (*B*) Rate of transducin activation by purified ancestral archosaur rhodopsin as measured by increases in fluorescence intensity (plotted in red), plotted against similarly treated bovine rhodopsin as a control (plotted in black). Fluorescence intensities are normalized to values at the time of GTPγS addition. Fluorescence of $G\alpha_t$ (250 nM), catalyzed by 1 nM rhodopsin in the presence of excess GTPγS, was monitored at 10°C using a SPEX spectrofluorometer equipped with a Xenon arc lamp by methods described previously (Marin et al. 2000).

DNA from exceptional samples preserved in amber or from dinosaur bone extracted from Cretaceous period coal beds have met with questionable success; in fact, material older than several hundred thousand years may not prove to be a reliable source of DNA, except under highly unusual circumstances (Hoss et al. 1996). An entirely different approach is to use phylogenetic methods to infer ancestral sequences (Yang, Kumar, and Nei 1995). One elegant study (Jermann et al. 1995) recreated in the laboratory the molecular evolution of ribonuclease, specifically in the artiodactyl lineage, whose ancestor was estimated to have lived approximately 40 MYA. These types of approaches combine phylogenetic inference of ancestral gene structure with gene synthesis methods to obtain biological molecules that can be characterized in detail to provide a better understanding of the biology of ancient animals.

Supplementary Material

The vertebrate rhodopsin alignment used to infer the sequence of an ancestral archosaur rhodopsin has been deposited in the EMBL alignment database (Accession number ALIGN_000323). The synthetic archosaur rhodopsin sequence has been deposited in GenBank (Accession number AF310191).

Acknowledgments

We thank Z. Yang, J. Bielawski, D. Campbell, R. L. Honeycutt, and three anonymous reviewers for their helpful comments and suggestions, and E. Marin for his help with the transducin fluorescence assay. This work was supported in part by the Howard Hughes Medical Institute, the Allene Reuss Memorial Trust, an NSF/Sloan Fellowship in Molecular Evolution (B.C.), and the Ellison Medical Foundation.

LITERATURE CITED

ADEY, N. B., T. O. TOLLEFSBOL, A. B. SPARKS, M. H. EDGELL, and C. A. HUTCHISON III. 1994. Molecular resurrection of an extinct ancestral promoter for mouse L1. Proc. Natl. Acad. Sci. USA **91**:1569–1573.

ARCHER, S., and J. HIRANO. 1996. Absorbance spectra and molecular structure of the blue-sensitive rod visual pigment in the conger eel (*Conger conger*). Proc. R. Soc. Lond. B **263**: 761–767.

ARCHER, S., A. HOPE, and J. C. PARTRIDGE. 1995. The molecular basis for the green-blue sensitivity shift in the rod visual pigments of the European eel. Proc. R. Soc. Lond. B **262**:289–295.

ARCHER, S. N., J. N. LYTHGOE, and L. HALL. 1992. Rod opsin cDNA sequence from the sand goby (*Pomatoschistus minutus*) compared with those of other vertebrates. Proc. R. Soc. Lond. B **248**:19–25.

BAEHR, J. F., J. D. FALK, K. BUGRA, J. T. TRIANTAFYLLOS, and J. F. MCGINNIS. 1988. Isolation and analysis of the mouse opsin gene. FEBS Lett. **238**:253–256.

BAYLOR, D. A., B. J. NUNN, and J. L. SCHNAPF. 1984. The photocurrent, noise and spectral sensitivity of rods of the monkey *Macaca fascicularis*. J. Physiol. **357**:575–607.

BISHOP, J. G., A. M. DEAN, and T. MITCHELL-OLDS. 2000. Rapid evolution in plant chitinases: molecular targets of selection in plant-pathogen coevolution. Proc. Natl. Acad. Sci. USA **97**:5322–5327.

BOISSINOT, S., Y. TAN, S. K. SHYUE, H. SCHNEIDER, I. SAMPAIO, K. NEISWANGER, D. HEWETT-EMMETT, and W. H. LI. 1998. Origins and antiquity of X-linked triallelic color vision systems in New World monkeys. Proc. Natl. Acad. Sci. USA **95**:13749–13754.

BOWMAKER, J. K., L. A. HEATH, S. E. WILKIE, and D. M. HUNT. 1997. Visual pigments and oil droplets from six clas-

ses of photoreceptor in the retinas of birds. Vision Res. **37**: 2183–2194.

Cao, Y., J. Adachi, T.-a. Yano, and M. Hasegawa. 1994. Phylogenetic place of guinea pigs: no support of the rodent-polyphyly hypothesis from maximum-likelihood analyses of multiple protein sequences. Mol. Biol. Evol. **11**:593–604.

Carroll, R. L. 1997. Patterns and processes of vertebrate evolution. Cambridge University Press, Cambridge.

Chandrasekharan, U. M., S. Sanker, M. J. Glynias, S. S. Karnik, and A. Husain. 1996. Angiotensin II–forming activity in a reconstructed ancestral chymase. Science **271**: 502–505.

Chang, B. S., M. A. Kazmi, and T. P. Sakmar. 2002. Synthetic gene technology: applications to ancestral gene reconstruction and structure-function studies of receptors. Methods Enzymol. **343**:274–294.

Chang, B. S. W., and M. J. Donoghue. 2000. Recreating ancestral proteins. Trends Ecol. Evol. **15**:109–114.

Cornwall, M. C., H. Ripps, R. L. Chappell, and G. J. Jones. 1989. Membrane current responses of skate photoreceptors. J. Gen. Physiol. **94**:633–647.

Crouch, R. 1976. Photosensitive pigments formed with rat opsin. Investig. Ophthalmol. **15**:872–875.

de Jong, W. W. 1998. Molecules remodel the mammalian tree. Trends Ecol. Evol. **13**:270–275.

Dean, A. M., and G. B. Golding. 1997. Protein engineering reveals ancient adaptive replacements in isocitrate dehydrogenase. Proc. Natl. Acad. Sci. USA **94**:3104–3109.

Felsenstein, J. 1981. Evolutionary trees from DNA sequences: a maximum likelihood approach. J. Mol. Evol. **17**:368–376.

Ferretti, L., S. S. Karnik, H. G. Khorana, M. Nassal, and D. D. Oprian. 1986. Total synthesis of a gene for bovine rhodopsin. Proc. Natl. Acad. Sci. USA **83**:599–603.

Fisher, P. E., D. A. Russell, M. K. Stoskopf, R. E. Barrick, M. Hammer, and A. A. Kuzmitz. 2000. Cardiovascular evidence for an intermediate or higher metabolic rate in an ornithischian dinosaur. Science **288**:503–505.

Fyhrquist, N., K. Donner, P. A. Hargrave, J. H. McDowell, M. P. Popp, and W. C. Smith. 1998*a*. Rhodopsins from three frog and toad species: sequences and functional comparisons. Exp. Eye Res. **66**:295–305.

Fyhrquist, N., V. Govardovskii, C. Leibrock, and T. Reuter. 1998*b*. Rod pigment and rod noise in the European toad *Bufo bufo*. Vision Res. **38**:483–486.

Gale, J. M., R. A. Tobey, and J. A. D'Anna. 1992. Localization and DNA sequence of a replication origin in the rhodopsin gene locus of Chinese hamster cells. J. Mol. Biol. **224**:343–358.

Galtier, N., N. Tourasse, and M. Gouy. 1999. A nonhyperthermophilic common ancestor to extant life forms. Science **283**:220–221.

Gauthier, J. A. 1994. The diversification of the amniotes. Pp. 129–159 *in* D. R. Prothero and R. M. Schoch, eds. Major features of vertebrate evolution: short courses in paleontology. The Paleontological Society, Knoxville, Tennesee.

Goldman, N., and Z. Yang. 1994. A codon-based model of nucleotide substitution for protein-coding DNA sequences. Mol. Biol. Evol. **11**:725–736.

Han, M., S. W. Lin, S. O. Smith, and T. P. Sakmar. 1996. The effects of amino acid replacements of glycine 121 on transmembrane helix 3 of rhodopsin. J. Biol. Chem. **271**: 32330–32336.

Harosi, F. I., and J. Kleinschmidt. 1993. Visual pigments in the sea lamprey, *Petromyzon marinus*. Vis. Neurosci. **10**: 711–715.

Hasegawa, M., H. Kishino, and T. Yano. 1985. Dating the human-ape splitting by a molecular clock of mitochondrial DNA. J. Mol. Evol. **22**:672–677.

Heath, L. A., S. E. Wilkie, J. K. Bowmaker, and D. M. Hunt. 1997. The rod and green cone opsins of two avian species, the budgerigar, *Melopsittacus undulatus*, and the mallard duck, *Anas platyrhynchus*. Gene **204**:121–126.

Hisatomi, O., T. Iwasa, F. Tokunaga, and A. Yaui. 1991. Isolation and characterization of lamprey rhodopsin cDNA. Biochem. Biophys. Res. Commun. **174**:1125–1132.

Hoss, M., P. Jaruga, T. H. Zastawny, M. Dizdaroglu, and S. Paabo. 1996. DNA damage and DNA sequence retrieval from ancient tissues. Nucleic Acids Res. **24**:1304–1307.

Huelsenbeck, J. P. 1997. Is the Felsenstein zone a fly trap? Syst. Biol. **46**:69–74.

Jermann, T. M., J. G. Opitz, J. Stackhouse, and S. A. Benner. 1995. Reconstructing the evolutionary history of the artiodactyl ribonuclease superfamily. Nature **374**:57–59.

Johnson, R. L., K. B. Grant, T. C. Zankel, M. F. Boehm, S. L. Merbs, J. Nathans, and K. Nakanishi. 1993. Cloning and expression of goldfish opsin sequences. Biochem. **32**:208–214.

Jones, D. T., W. R. Taylor, and J. M. Thornton. 1992. The rapid generation of mutation data matrices from protein sequences. Comput. Appl. Biosci. **8**:275–282.

Kawamura, S., N. S. Blow, and S. Yokoyama. 1999. Genetic analyses of visual pigments of the pigeon (*Columba livia*). Genetics **153**:1839–1850.

Kawamura, S., and S. Yokoyama. 1998. Functional characterization of visual and nonvisual pigments of American chameleon (*Anolis carolinensis*). Vision Res. **38**:37–44.

Koskelainen, A., P. Ala-Laurila, N. Fyhrquist, and K. Donner. 2000. Measurement of thermal contribution to photoreceptor sensitivity. Nature **403**:220–223.

Kylma, T., C. Roos, L. Paulin, and B. Kommonen. 1997. The introns of the canine rod opsin gene show higher sequence homology to the human than to the rodent introns. DNA Seq. **8**:99–104.

Lythgoe, J. N. 1972. List of vertebrate visual pigments. Pp. 604–623 *in* H. J. A. Dartnall, ed. Photochemistry of vision. Springer-Verlag, New York.

Makino, C. L., M. Groesbeek, J. Lugtenburg, and D. A. Baylor. 1999. Spectral tuning in salamander visual pigments studied with dihydroretinal chromophores. Biophys. J. **77**:1024–1035.

Malcolm, B. A., K. P. Wilson, B. W. Matthews, J. F. Kirsch, and A. C. Wilson. 1990. Ancestral lysozymes reconstructed, neutrality tested, and thermostability linked to hydrocarbon packing. Nature **345**:86–89.

Marin, E. P., A. G. Krishna, T. A. Zvyaga, J. Isele, F. Siebert, and T. P. Sakmar. 2000. The amino terminus of the fourth cytoplasmic loop of rhodopsin modulates rhodopsin-transducin interaction. J. Biol. Chem. **275**:1930–1936.

Menon, S. T., M. Han, and T. P. Sakmar. 2001. Rhodopsin: structural basis of molecular physiology. Physiol. Rev. **81**: 1659–1688.

Messier, W., and C. B. Stewart. 1997. Episodic adaptive evolution of primate lysozymes. Nature **385**:151–154.

Muse, S. V., and B. S. Gaut. 1994. A likelihood approach for comparing synonymous and nonsynonymous nucleotide substitution rates, with application to the chloroplast genome. Mol. Biol. Evol. **11**:715–724.

Nathans, J., and D. S. Hogness. 1983. Isolation, sequence analysis, and intron-exon arrangement of the gene encoding bovine rhodopsin. Cell **34**:807–814.

NATHANS, J., D. THOMAS, and D. S. HOGNESS. 1984. Isolation and nucleotide sequence of the gene encoding human rhodopsin. Proc. Natl. Acad. Sci. USA **81**:4851–4855.

NAVIDI, W. C., G. A. CHURCHILL, and A. VON HAESELER. 1991. Methods for inferring phylogenies from nucleic acid sequence data by using maximum likelihood and linear invariants. Mol. Biol. Evol. **8**:128–143.

NEI, M., J. ZHANG, and S. YOKOYAMA. 1997. Color vision of ancestral organisms of higher primates. Mol. Biol. Evol. **14**: 611–618.

NICKELLS, R. W., C. F. BURGOYNE, H. A. QUIGLEY, and D. J. ZACK. 1995. Cloning and characterization of rod opsin cDNA from the Old World monkey, *Macaca fascicularis*. Investig. Ophthalmol. Vis. Sci. **36**:72–82.

O'BRIEN, J., H. RIPPS, and M. R. AL-UBAIDI. 1997. Molecular cloning of a rod opsin cDNA from the skate retina. Gene **193**:141–150.

PALCZEWSKI, K., T. KUMASAKA, T. HORI et al. (12 co-authors). 2000. Crystal structure of rhodopsin: a G protein-coupled receptor. Science **289**:739–745.

PITTLER, S. J., S. J. FLIESLER, and W. BAEHR. 1992. Primary structure of frog rhodopsin. FEBS Lett. **313**:103–108.

RUBEN, J. A., C. DAL SASSO, N. R. GEIST, W. J. HILLENIUS, T. D. JONES, and M. SIGNORE. 1999. Pulmonary function and metabolic physiology of theropod dinosaurs. Science **283**: 514–516.

SAHA, M. S., and R. M. GRAINGER. 1993. Early opsin expression in *Xenopus* embryos precedes photoreceptor differentiation. Mol. Brain Res. **17**:307–318.

SCHNAPF, J. L., T. W. KRAFT, B. J. NUNN, and D. A. BAYLOR. 1988. Spectral sensitivity of primate photoreceptors. Vis. Neurosci. **1**:255–261.

SMITH, W. C., G. ADAMUS, H. VAN DER WEL, A. TIMMERS, K. PALCZEWSKI, R. J. ULSHAFER, P. A. HARGRAVE, and J. H. MCDOWELL. 1995*a*. Alligator rhodopsin: sequence and biochemical properties. Exp. Eye Res. **61**:569–578.

SMITH, W. C., J. M. MARTINKO, J. N. WHEELER, P. A. HARGRAVE, and J. H. MCDOWELL. 1995*b*. The deduced aminoacid sequence of opsin from rabbit rod photoreceptors. Gene **162**:331–332.

STRYER, L. 1986. Cyclic GMP cascade of vision. Ann. Rev. Neurosci. **9**:87–119.

SULLIVAN, J., and D. L. SWOFFORD. 1997. Are guinea pigs rodents? The importance of adequate models in molecular phylogenetics. J. Mamm. Evol. **4**:77–86.

TAKAO, M., A. YASUI, and F. TOKUNAGA. 1988. Isolation and sequence determination of the chicken rhodopsin gene. Vision Res. **28**:471–480.

TSAI, H. J., S. R. SHIH, C. M. KUO, and L. K. LI. 1994. Molecular cloning of the common carp (*Cyprinus carpio*) rhodopsin cDNA. Comp. Biochem. Physiol. B Comp. Biochem. Mol. Biol. **109**:81–88.

VIHTELIC, T. S., C. J. DORO, and D. R. HYDE. 1999. Cloning and characterization of six zebrafish photoreceptor opsin cDNAs and immunolocalization of their corresponding proteins. Vis. Neurosci. **16**:571–585.

YANG, Z. 1994. Estimating the pattern of nucleotide substitution. J. Mol. Evol. **39**:105–111.

YANG, Z. 1997. PAML: a program package for phylogenetic analysis by maximum likelihood. Comput. Appl. Biosci. **13**: 555–556.

YANG, Z., N. GOLDMAN, and A. FRIDAY. 1994. Comparison of models for nucleotide substitution used in maximum-likelihood phylogenetic estimation. Mol. Biol. Evol. **11**:316–324.

YANG, Z., S. KUMAR, and M. NEI. 1995. A new method of inference of ancestral nucleotide and amino acid sequences. Genetics **141**:1641–1650.

YOKOYAMA, R., B. E. KNOX, and S. YOKOYAMA. 1995. Rhodopsin from the fish, *Astyanax*: role of tyrosine 261 in the red shift. Investig. Ophthalmol. Vis. Sci. **36**:939–945.

YOKOYAMA, S., N. S. BLOW, and F. B. RADLWIMMER. 2000. Molecular evolution of color vision of zebra finch. Gene **259**:17–24.

ZHANG, H., and S. YOKOYAMA. 1997. Molecular evolution of the rhodopsin gene of marine lamprey, *Petromyzon marinus*. Gene **191**:1–6.

RODNEY HONEYCUTT, reviewing editor

Accepted May 2, 2002